

Using Multiple Information Sources to Construct Stochastic Databases to Quantify Uncertainty in Certification Maneuvers

Andrew D. Wendorff*, and Juan J. Alonso†

Stanford University, Stanford, CA 94305, USA

Stefan R. Bieniawski‡

Boeing Research & Technology, Seattle, WA, 98124

Understanding how a new aircraft configuration will perform during certification maneuvers is important during the conceptual design phase. Most current methodologies require a complete aerodynamic database be constructed without a way to determine how the uncertainty in the database affects the resulting maneuvers. Building upon previous work in combining multiple information sources to build a stochastic aerodynamic database for the configuration of interest, this paper contains a methodology to estimate what location in the flight envelope has the dominant impact on the uncertainty in the quantity of interest. This is done by estimating the aerodynamic characteristics at a set of Latin Hypercube Sampling locations. The maneuver is then run multiple times using deterministic samples of the stochastic database incorporating each of the LHS locations separately. Fitting a Gaussian Process between the vehicle conditions (angle of attack (α), Mach number, control surface deflection, etc.) and the quantity of interest (a measure of the uncertainty in the maneuver), we found the best results could reduce the 90% Confidence Interval of the time to descend in the emergency descent case by approximately 70% when adding 5 new high fidelity points.

I. Introduction

During the conceptual and preliminary aircraft design phases, there is often a need to estimate both the static and dynamic responses of the vehicle. These characteristics are used as a way to estimate the necessary Stability and Control (S&C) requirements that govern control surface location, sizing, and range of motion to generate the necessary forces and moments to conduct all certification maneuvers. While aerodynamics, propulsion, and weights receive most of the attention in the design of new vehicles, S&C requirements and control surface sizing are relegated to simplistic constraints or correlations based on previous aircraft. It is not until later in the design process where an in-depth understanding of S&C characteristics and their effective on vehicle performance is obtained. To estimate certification requirements, aerodynamic databases (containing force and moment coefficients with respect to flight condition, angular rate, control surface deflection, etc.) of the design need to be generated and trajectory simulations run to determine if the configuration meets the certification requirements. These deterministic databases are typically estimated from a single information source corresponding to the current design phase. This database could, however, combine multiple pieces of aerodynamic information coming from a number of different information sources (including wind-tunnel and flight testing) with varying associated costs, fidelity levels, lead times, and uncertainties.

The new stochastic database created contains an inexact estimate of the forces and moments generated on the vehicle at different flight conditions. By combining multiple sources of aerodynamic data, we can focus the more expensive and accurate analysis tools into area of the flight envelope where small errors can lead to large changes in vehicle performance. At present, these higher accuracy analysis techniques are only

*Graduate Student, Department of Aeronautics and Astronautics, AIAA Student Member.

†Professor, Department of Aeronautics and Astronautics, AIAA Associate Fellow.

‡Technical Fellow, Senior Member AIAA.

applied to a vehicle when the configuration is primarily set since it is prohibitively expensive to populate the database for a rapidly changing design. Once the configuration has been fixed, the opportunity to make slight changes in the design that significantly improve the probability of meeting certification requirements has been lost. Boeing used the 787-8 as a high fidelity analysis surrogate when readying the 787-9 for testing and certification in order to improve vehicle prediction over a year before the first 787-9 took flight.¹ In addition to potentially modifying the aircraft design, pushing S&C analysis further forward in the design phase allows control systems to be better integrated into the system enabling additional capabilities and improving performance instead of fixing problems.

Moving S&C analysis techniques further forward in the design process is not as easy as using the same methodologies the same way, just earlier. It is too expensive to run very accurate information sources over the entire flight envelope for a vehicle in the conceptual design phase. There are a multitude of methods to compute the data contained in aerodynamic databases, but no formal procedure to determine, for a desired level of accuracy/uncertainty, which tool to use when, and in what region of the flight envelope. In our previous work,² we constructed a mathematical framework capable of combining multiple information sources to generate a stochastic database. We then integrated this stochastic database into a maneuver of interest, emergency descent, to see how the effect of uncertainty in the aerodynamic model would impact the likelihood of meeting the certification requirements. This work also showed how if additional analysis points are chosen intelligently, the uncertainty in a maneuver can be dramatically reduced. No methodology was presented to identify these points intelligently though.

In this work, we will present a potential solution to determine what location should be sampled next to reduce the uncertainty, our Quantity of Interest (QoI), as rapidly as possible. Additionally, we will consider how the uncertainty in the vehicle characteristics affects our methodology. Section II contains the background information on our problem from our previous work.² This includes the general optimization formulation, integration framework, stochastic aerodynamic database implementation, certification maneuver, and reference vehicle. In Section III, we explain how the uncertainty in our methodology is propagated from adding a new sampling location to the maneuver QoI. Since we are not trying to improve a characteristic of the aerodatabase as is typically done, but instead reduce the uncertainty in a maneuver, we have found a numerical solution. In Section IV, we explain our procedure to estimate the optimal sampling point to reduce some uncertainty measure of the maneuver QoI. The results we obtained from implementing this procedure to add high fidelity points, along with the effects of uncertainty in the underlying vehicle are in Section V. Finally, a summary of our methodology and results are found in Section VI.

II. Problem Background

The primary focus of this work is to look at an optimal allocation problem focused on moving stability and control analysis further forward in the process for designing aircraft. To do this, we formulated the optimization procedure, created an integrated framework to pass information, and constructed a stochastic database over an emergency descent flight envelope for the National Aeronautics and Space Administration (NASA) Common Research Model (CRM).²

A. Optimization Formulation

To meet our ultimate objective, we must efficiently combine data from multiple information sources to manage uncertainty. Sampling the right fidelity level at the right location is important to optimally allocate the resources available. Depending on the objective, minimum uncertainty or minimum cost, the quantity of interest and constraints change.

1. Minimizing the Uncertainty in Aircraft Simulation

In the first formulation, the end user desires to minimize some QoI (q) of the distribution $Z(\mathbf{z}_p^1, \dots, \mathbf{z}_p^k)$ for maneuver p where each \mathbf{z}_p^k is a function of all the samples \mathbf{x}^1 through \mathbf{x}^k of the information sources. q could be the variance in the distribution, a confidence interval, an acceptable error, or another deterministic measure of the maneuvers. $h(Z(\mathbf{z}_t^1, \dots, \mathbf{z}_t^{kk}), F_i^j(\mathbf{x}_i))$ denotes a constraint over maneuver t that must be satisfied when $F_i^j(\mathbf{x}_i)$ is the stochastic function of aerodynamic coefficient j for information source i . One of the other possible constraints placed on this optimization procedure is the total computational budget available. This situation is representative of the requirement that our methodology meets the rapid design

environment where a vehicle needs to be studied quickly and feedback provided because configurations are always changing. The formal mathematical optimization set up for this problem is

$$\begin{aligned}
& \underset{\mathbf{x}^{k+1}}{\text{minimize}} && q(\mathbf{x}_{ii}^1, \dots, \mathbf{x}_{jj}^k) \\
& \text{subject to} && h_{iii}(Z(\mathbf{z}_t^1, \dots, \mathbf{z}_t^{kk}), F_i^j(\mathbf{x}_i)) \leq 0 \quad iii \in \{1, \dots, tt\} \\
& && \sum_{i=1}^m c_i n_i \leq \mathbb{C} \\
& && lb_{jjj} \leq x_{jjj} \leq ub_{jjj}, \quad jjj \in \{1, \dots, r\} \\
& && \mathbf{x}^{k+1} \in \mathbb{R}^r
\end{aligned} \tag{1}$$

where in \mathbf{x}_{jj}^k , the superscript denotes the sample number with k being the last analyzed location and the subscript denotes the fidelity level used to evaluate the sample. r is the dimension of possible vehicle conditions incorporating all flight conditions, control surface deflections, pitch rates, etc. c_i is the relative cost of analysis i compared to the other information sources, n_i is the number of times that single methodology is used, and \mathbb{C} is the total computational budget. tt is the total number of constraints and m is the total number of information sources being used.

2. Minimizing Computational Cost

The second way we set up the problem builds constraints to specify the uncertainty necessary from the S&C characteristic of interest with the objective to minimize computational cost to meet the requirement. This formulation is indicative of a slightly later step in the vehicle design process where, instead of trying to quickly analyze as many configurations as possible, the objective is to satisfy all the desired uncertainty requirements by using a set of maneuvers to estimate a total probability the vehicle will be certified. These conditions manifest themselves as constraints (h 's) on the performance metric defined by

$$\begin{aligned}
& \underset{\mathbf{x}^{k+1}}{\text{minimize}} && \sum_{i=1}^m c_i n_i \\
& \text{subject to} && q(\mathbf{x}_{ii}^1, \dots, \mathbf{x}_{jj}^k) - q_{max} \leq 0 \\
& && h_{iii}(Z(\mathbf{z}_t^1, \dots, \mathbf{z}_t^{kk}), F_i^j(\mathbf{x}_i)) \leq 0 \quad iii \in \{1, \dots, tt\} \\
& && lb_{jjj} \leq x_{jjj} \leq ub_{jjj}, \quad jjj \in \{1, \dots, r\} \\
& && \mathbf{x}^{k+1} \in \mathbb{R}^r
\end{aligned} \tag{2}$$

where q_{max} is the maximum allowed value of the QoI that is partially driving the number of samples necessary. These two situations do not have to be mutually exclusive, our methodology can be extended to a situation where there is a set computational limit integrated with a required performance characteristic on the output parameter.

B. Integration Framework

Once we have formulated the optimization problem of interest, we need to incorporate the actual maneuvers and information sources needed to analyze the configuration through the maneuvers. Multiple pieces of information must be specified including:

- Aircraft Characteristics
- Information Sources
- Database Construction Method
- Certification Maneuvers
- Uncertainty Quantification (UQ) Methodology
- Maneuver Approval Measure
- Quantity of Interest

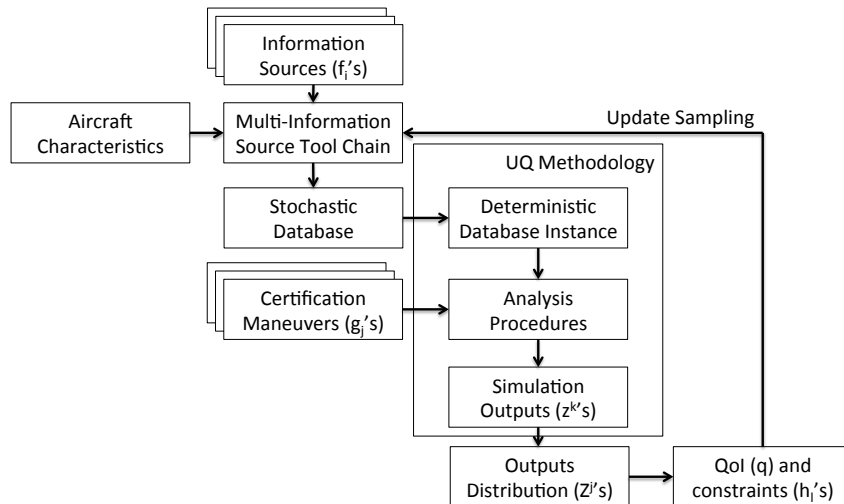


Figure 1: Connection between Components to Analyze Configuration for Certification Maneuvers²

The integration of these different inputs into a mathematical analysis component is shown in Figure 1.

In our analysis, we require the physical characteristics of the aircraft be an input.² Any design change that would affect the aerodynamic output from one of the information sources is fixed in this part of the design evaluation. If a aircraft parameter does not affect the information sources, then it is free to be a stochastic parameter. The information sources are treated as a set of “black-box” functions where the inputs are provided and the outputs generated with no modifications to the underlying code. We slightly simplify the problem, at present, by assuming the most accurate information source is the “truth” model so we are not focusing on the model-form uncertainty problem. Once we have created this multi-information source tool chain, we are able to create a stochastic database containing the best estimate of the underlying variable, typically the mean, and a measure of the uncertainty in that parameter, the variance for instance. This stochastic database of the aircraft is used with UQ techniques to simulate certification maneuvers. We can then generate statistics to measure the probability of meeting certification requirements and calculate the QoI.²

C. Stochastic Database

Our previous paper² discussed in detail the development of the stochastic database. We are only using two information sources at present to focus on the algorithm for determining where a new sample should be added. We simplify the methodology by saying the low fidelity results can be called infinitely less expensively than the high fidelity. This assumption removes the requirement to create a separate response surface for the lower fidelity level. To create the stochastic database, we have to

1. Determine locations to sample each of the information sources $\mathbf{x}_1^1, \dots, \mathbf{x}_1^k$ for $i = 1, \dots, m$.
2. Combine the deterministic outputs, $f_i^j(\mathbf{x}_i^k)$, of each information source into $F_i^j(\mathbf{x})$ to span \mathbb{R}^r .
3. Incorporate a combinatoric strategy to adjust lower fidelity levels to $F_0^j(\mathbf{x})$, the highest fidelity level.

For our initial sampling of the design space, we used a Latin Hypercube Sampling (LHS) methodology for the highest fidelity level as it generates a better result than a lattice approach. We are constructing our response surface using the DACE Toolbox in MATLAB.³ For fidelity level i , the surface is constructed using:

$$F_i(\mathbf{x}) = \mathbf{b}_i(\mathbf{x})^T \beta_i + \mathbb{Z}_i(\mathbf{x}) \quad (3)$$

where \mathbf{b}_i and β_i are the basis functions and the coefficients, respectively, of a linear model. \mathbb{Z}_i is modeled as a zero-mean stationary Gaussian stochastic process with covariance between points \mathbf{x} and \mathbf{x}' calculate as $\sigma_{\mathbb{Z},i}^2 \mathbf{R}$. $\sigma_{\mathbb{Z},i}^2$ is the signal variance and \mathbf{R} , we assume, is a Gaussian correlation:

$$\mathbf{R} = \text{Corr} [\epsilon_i(\mathbf{x}), \epsilon_i(\mathbf{x}')] = \prod_{j=1}^r \exp [-\theta_j (x_j - x'_j)^2] \quad (4)$$

where r is the dimension the response surface covers and θ_j is the hyper-parameter associated with a specific dimension j . The possible aerodynamic characteristic at each possible vehicle state is modeled by a normal random variable with mean μ and variance σ^2 . This response surface is commonly known as a Gaussian Process (GP). To combine the multiple fidelity levels into one stochastic database, we will use a additive combinatorial strategy

$$F_{l(j)}^j(\mathbf{x}) = F_{l(j)+1}^j(\mathbf{x}) + \alpha_{l(j)}^j(\mathbf{x}) \quad (5)$$

where $l(j)$ is some subset of information sources i that provide information for quantity of interest j over the the design space modifying the work of Huang et al. (2006).⁴ In our case, the low fidelity is thus called at any point needed to be analyzed and the actual vehicle forces and moment are determined using the GP of the additive correction for each term of interest.

Within our methodology, we decided to maintain correlation among aerodynamic coefficients by taking the stochastic database and sampling at the location of interest using a multivariate normal constructed from all the different characteristics stored in our database. To calculate the covariance matrix Σ for the multivariate normal, we must estimate the correlation between stochastic coefficients stored in the aerodynamic database. The correlation between parameters is calculated using the sample correlation function:

$$\rho(\mathbf{y}_j, \mathbf{y}_k) = \frac{\frac{1}{n_0-1} \sum_{i=1}^{n_0} ((y_{j,i} - \mu_j)(y_{k,i} - \mu_k))}{\sigma_j \sigma_k} \quad (6)$$

where μ_j denotes the mean value from the high fidelity information source of characteristic j over the entire aerodynamic database, σ_j denotes the estimated standard deviation of these results, and n_0 is the number of “truth” samples. Once one set of deterministic samples \mathbf{y}^i of the stochastic database has been calculated from the multivariate Gaussian at the flight condition of interest, a conditional updating procedure is followed. Coefficients at additional flight conditions are then found with the multivariate Gaussian conditioned on the deterministic instances generated at previous flight conditions sampled. The procedure is repeated, updating the conditional distribution, until deterministic instances of the stochastic database are generated for all conditions necessary to simulate the maneuvers of interest. In one dimension, this methodology is illustrated in Figure 2.

The shaded area in Figure 2 shows the possible data values falling within two standard deviations of the response surface mean. The black dotted line, our deterministic function, in Figure 2 is one of the possible estimates of the true underlying function, denoted as the green line, which is unknown. This methodology removes the requirement that an entire deterministic aerodynamic database be stored to run maneuvers of interest. With this methodology in place to instance the stochastic database constructed using Gaussian Processes, we have the capability to analyze aircraft through specific certification maneuvers while retaining uncertainty in the underlying design. We can then propagate uncertainty to determine potential problem areas.

D. Emergency Descent

The emergency descent maneuver requires the spoilers create as much drag as possible so the aircraft can descend as rapidly as possible. The maximum drag is related to the maximum deflection of the spoiler for a prescribed maximum torque or corresponding hinge moment.

1. Requirements

The emergency descent maneuver, as written into FAR 25.841 related to cabin pressures, requires that if an aircraft wants to be certified above 25,000 ft, then “the airplane must be designed so occupants will not be

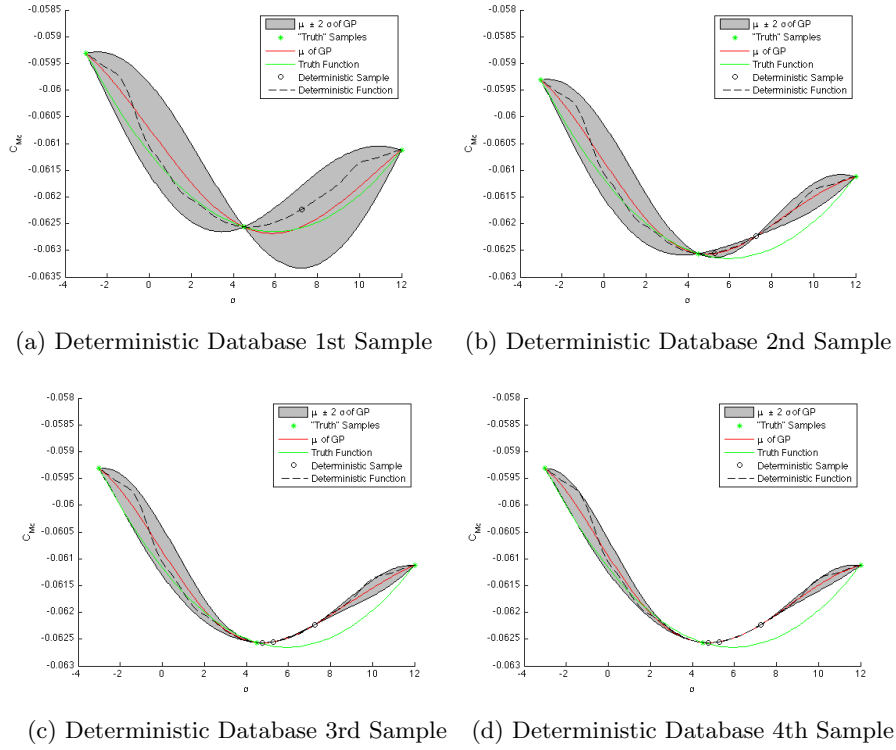


Figure 2: Constructing a Deterministic Aerodynamic Database²

exposed to cabin pressure altitude that exceeds the following after decompression from any failure condition not shown to be extremely improbable:

1. Twenty-five thousand (25,000) feet for more than 2 minutes; or
2. Forty thousand (40,000) feet for any duration.”⁵

This requirement is one that helps guide the aircraft designers to determine the maximum cruise altitude of the aircraft. Instead of using the cabin pressure altitude for our study, we instead use the aircraft altitude as this should be a conservative estimate of the cabin altitude.

2. Trajectory Analysis

When this maneuver is conducted in general, there are three major segments between which the aircraft transitions. The aircraft starts in the trim cruise condition when a warning alerts the pilots to a cabin depressurization. At that time, the pilots pitch the aircraft over and trims the vehicle to descend at M_{MO} , the maximum operating Mach number of the aircraft. During the descent profile, the aircraft reaches a transition altitude where the aircraft must retrim at V_{MO} , the maximum operating velocity. The vehicle continues to descend at this condition until the aircraft descends below 25,000 ft at which time the clock stops. The aircraft, however, continues to descend down to a lower cruise altitude of 10,000 or 15,000 ft. Since the maneuver after the aircraft altitude decreases below 25,000 ft is not part of the certification requirement, we are not concerned with this portion of the trajectory in our analysis. As a way to avoid doing a complete non-linear simulation of the maneuver, which can be quite expensive, we instead are using control point analysis where we discretize the descent profile into a fixed set of locations defined by an altitude and Mach number. The aircraft must then be trimmed at each of these locations by querying the stochastic database.

To trim the aircraft, we are using the set of equations based on the work of Stevens and Lewis.⁶ An inner sizing loop is used to match the spoiler torque to the maximum specified torque for each of the spoilers. The maximum torque will equal the maximum blow-back force generated by the airflow over the aircraft.

Assuming a triangular pressure profile over the spoiler following the work of Stoecklin,⁷ the torque of the spoiler is

$$\tau_s = \frac{b_s c_s^2 S_w \bar{q} \sqrt{\Delta C_{D_{\delta_s}}^2 + \Delta C_{L_{\delta_s}}^2} \delta_s}{3 S_s} \quad (7)$$

where δ_s is the spoiler deflection, \bar{q} is the dynamic pressure at the control point of interest, and $\Delta C_{D_{\delta_s}}$ and $\Delta C_{L_{\delta_s}}$ are the changes in drag and lift, respectively, as discussed previously.² We had previously assumed the maximum spoiler torque was fixed for all the trajectories considered. In this paper, Section V contains a study of how uncertainty in vehicle characters including mass and moment of inertia, throttle setting, and maximum spoiler torque impact the time to descend.

E. NASA CRM

Our methodology does not create new configurations. We instead analyze designs created by other engineers. As such, we have used the NASA CRM as our test vehicle. The NASA CRM configuration was developed to be used in a CFD (Computational Fluid Dynamics) validation exercise as part of the fourth AIAA (American Institute of Aeronautics and Astronautics) CFD Drag Prediction Workshop.⁸ This is a high-speed configuration where the geometry is widely available and studied extensively. The reference quantities for the CRM main wing are located in Table 1 where λ is the taper ratio and the X, Y, Z reference locations are for half the main wing, not the entire vehicle. The horizontal tail, with characteristics shown in Table 2, is designed to be robust at dive Mach number conditions was added for stability and control considerations.

Table 1: Reference Quantities for the CRM main wing⁸

Sref	594,720.0 in ²	4,130.0 ft ²
Cref	275.8 in	
Span	2,313.5 in	192.8 ft
Xref	1,325.9 in	
Yref	468.75 in	
Zref	177.95 in	
λ	0.275	
$\Lambda_{C/4}$	35°	
AR	9.0	

Table 2: Reference Quantities for the CRM Horizontal Tail

Sref	144,000.0 in ²	1,000.0 ft ²
Cref	184.7 in	
Span	840 in	70 ft
λ	0.35	
$\Lambda_{C/4}$	37°	

We have chosen to use the horizontal tail configuration with horizontal tail incidence angle ($i_h = 0^\circ$). The CRM is not designed with control surfaces or vertical tail so a vertical tail, elevator, and spoilers based on Boeing 777-200⁹ as discussed previously² are integrated into the aircraft evaluated. The control surface characteristics are shown in Table 3.

The CRM does not have a defined mass or moment of inertia. As these parameters are necessary for our analysis, we will assume the CRM mass is 545,000 lbs, the same as the Boeing 777-200⁹, and the moment of inertia I_{yy} is estimated at $2.4e7 \text{ slugs} - ft^2$. We also assume the CRM has two 77,000 lbs thrust engines in the same locations as the Boeing 777-200. This geometry was then analyzed by QuadAir¹⁰ and a compilation of handbook methods² to create the stochastic aerodynamic database over the design space of interest. This

Table 3: CRM Longitudinal Control Surfaces Based on the Boeing 777-200²

$c_{\delta e}/c_h$	0.2849
$Span_{\delta e}$	524.7 in ²
n_{spoil}	5
$Span_{spoil}$	84.12 in
$Creff_{spoil}$	21.05 in

stochastic database was analyzed using a Monte Carlo UQ analysis technique to determine how the aircraft would complete the maneuvers of interest.

III. Propagating Uncertainty from Additional Sampling Location to Quantity of Interest

In order to be able to optimally place points to reduce some QoI, the connection between an additional sampling location and the specified QoI needs to be determined. The uncertainty in time to reach 25,000 ft for the emergency descent maneuver is a good QoI as designers are interested in the probability the vehicle will meet the 120 second time limit. Our new optimization formulation based on the generalized framework shown in Section II is

$$\begin{aligned}
 & \underset{\Delta \mathbf{x}^k}{\text{minimize}} && \sigma^2(t_D) \\
 & \text{subject to} && n_{HI-FID} = K \\
 & && lb_{jjj} \leq x_{jjj} \leq ub_{jjj}, \quad jjj \in \{1, \dots, r\} \\
 & && \mathbf{x}^{k+1} \in \mathbb{R}^r
 \end{aligned} \tag{8}$$

where $\Delta \mathbf{x}^k = [\bar{\mathbf{x}}^k; \mathbf{x}^{k+1}]^T$ denotes adding one additional sample to already evaluated $\bar{\mathbf{x}}^k$ terms and K is the total number of high fidelity samples able to be added. We assumed the low fidelity is infinitely less expensive than the high fidelity in this case. We can use the variance as a measure of this uncertainty and the connection to adding a new sampling location can be broken out as follows

$$\frac{\Delta \sigma^2(t_D)}{\Delta \mathbf{x}^k} = \left(\frac{\Delta \sigma^2(t_D)}{\Delta t_{D_j}} \right) \left(\frac{\Delta t_{D_j}}{\Delta t_j} \right) \left(\frac{\Delta t_j}{\Delta \gamma_j} \right) \left(\frac{\Delta \gamma_j}{\Delta \mathbf{x}_{trim}} \right) \left(\frac{\Delta \mathbf{x}_{trim}}{\Delta d(\bar{\mathbf{x}}^k)} \right) \left(\frac{\Delta d(\bar{\mathbf{x}}^k)}{\Delta D(\bar{\mathbf{x}}^k)} \right) \left(\frac{\Delta D(\bar{\mathbf{x}}^k)}{\Delta \mathbf{x}^k} \right) \tag{9}$$

Now, we can work backwards calculating how the uncertainty measure in time to descend is impacted by the change in one sample, $\frac{\Delta \sigma^2(t_D)}{\Delta t_{D_i}} = \frac{2t_{D_j} - \bar{\mu}_{t_D}}{N}$. This process can continue incorporating terms such as $\frac{\Delta t_j}{\Delta \gamma_j} = \frac{\Delta h_j}{V_{T_j} \sqrt{1 - \gamma_j^2}}$ to determine the descent time in comparison to the flight path angle.

However, trying to determine $\frac{\Delta d(\bar{\mathbf{x}}^k)}{\Delta D(\bar{\mathbf{x}}^k)}$, the change in the deterministic sample $d(\bar{\mathbf{x}}^k)$ with the change in the underlying stochastic database $D(\bar{\mathbf{x}}^k)$ is inherently uncertain and will require sampling. Beyond that term, we also have an optimization where instead of changing one point, we are adding flight conditions to an already established set of points that continues growing. In addition, our function allows the sampling location order to be flipped because the Gaussian Process does not change based on the order of data. The change in the trim condition \mathbf{x}_{trim} with respect to changing databases must also be taken into account. All these non-standard characteristics of our function of interest, $\frac{\Delta \sigma^2(t_D)}{\Delta \mathbf{x}^k}$, direct us towards an computational algorithm instead of a closed-form analytic solution.

IV. Sampling Methodology

Once it was determined an analytic solution was not feasible for this type of problem, a numerical solution seemed to be the best option. Instead of using some sort of bin structure discretizing the domain and then randomly sampling inside the bin following the work of Tang et al.,¹¹ we wanted the algorithm to produce a single point to improve the aerodynamic database. The procedure used to generate this next sampling point is:

1. Sample different information sources at their corresponding LHS locations.
2. Build the stochastic database using the procedure outlined in Section II.
3. Create a second LHS set of locations where a single high fidelity point could be added.
4. Assume mean of the GP is the high fidelity solution for one of the locations from the second LHS set.
5. Update the Stochastic Database with this information.
6. Run a Monte Carlo analysis of the maneuver of interest for this new database, obtaining the QoI for this new database.
7. Repeat the process using the different locations contained in the second LHS until all locations have been used and have a corresponding QoI measure.
8. Create a GP over the QoI at the different locations from the second LHS set using the Monte Carlo results from the stochastic database with mean added at the one specified location.
9. Run a genetic algorithm over the QoI GP using a specified objective function to determine the next location to add a high fidelity point.

This procedure will add one high fidelity sample in the case where the low fidelity is extremely cheap to run and the high fidelity is much more expensive. We use the DACE toolbox³ to create all the GP surfaces. The genetic algorithm used is the `ga` function in MATLAB for an unconstrained minimization with a population size of 40.

While this methodology does produce an estimate of the best point to choose in order to reduce the QoI as much as possible, there are some decisions that must be made. The three major choices are

- How many potential high fidelity locations to include in the second LHS set?
- How many Monte Carlo samples to run of the maneuver of interest to estimate the QoI?
- What objective function to use to determine the next high fidelity point?

Considering the number of locations in the second LHS set and the number of Monte Carlo samples to run the maneuver through, the greater the number of both locations and MC samples, the greater the reduction in the uncertainty of the maneuver of interest. As seen in Table 5 located in Section V, this is the general trend. A more interesting question is if there is a fixed number of times the simulation can be run before the maneuver simulation costs become more expensive than just running the high fidelity information source, how do we determine the optimal split between more LHS locations and more samples at each particular location. Our results for this study are shown in Section V.

When trying to determine what objective function to use, there is the possibility to use the mean of the GP or the mean minus some constant times the standard deviation to find the point. There is also the option to use a different objective such as expected improvement (EI) developed by Jones et al.¹² The expected improvement function combines the mean and standard deviation of the GP with the current best function value using

$$E[I(\mathbf{x})] = (f_{min} - \hat{y})\Phi\left(\frac{f_{min} - \hat{y}}{s}\right) + s\phi\left(\frac{f_{min} - \hat{y}}{s}\right) \quad (10)$$

where ϕ and Φ are the standard normal density and distribution function, respectively. f_{min} in our case is the current minimum QoI seen not accounting for any of the locations from the second LHS set. A comparison of different objective functions with differing number of locations and samples at those locations is contained in Section V.

V. Results

Now that we have created this new methodology to find the best flight condition to sample at high fidelity in order to reduce the QoI as significantly as possible, we need to test its effectiveness. We do not only want to look at a vehicle that is fixed, but potentially one that incorporates uncertainties in different components as outlined in Section II. As such we will first cover the optimization of a vehicle with fixed characteristics and only an uncertain aerodatabase. After seeing how our algorithm works in the deterministic characteristic case, we will compare descent times when adding uncertainties in mass, moment of inertia, throttle setting, and maximum torque. Finally, we will see how our algorithm performs on a stochastic vehicle.

A. Deterministic Characteristic Vehicle Optimization

The baseline vehicle we start with uses a throttle setting of 0.15, maximum torque of 5.5e3 ft-lbs, V_{MO} equal to 900 ft/s, and M_{MO} equal to 0.9072. The histogram of time to descend for this vehicle with the stochastic database created from 10 high fidelity data points is shown in Figure 3.

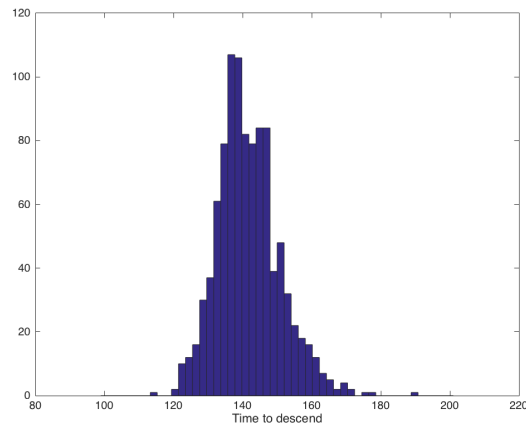


Figure 3: Time to Descend Histogram of CRM in Emergency Descent Maneuver

This configuration, with its corresponding stochastic database, results in a standard deviation of the maneuver time to descend of 9.1273 seconds from 1000 Monte Carlo samples. We decided to use the EI objective for our optimization over the surface build using 50 different LHS locations with 10 samples at each location to calculate the QoI. 12 high fidelity points were added to try to reduce the QoI. Figure 4 shows how the standard deviation in time to descend reduces with adding new high fidelity points.

Since EI requires f_{min} to be known as part of the objective function, we used 100 samples after adding each high fidelity point to estimate the standard deviation of time to descend and then 10,000 Monte Carlo samples at the end to get a good estimate of the actual standard deviation. We see in Figure 4 that by adding 12 additional high fidelity points, the standard deviation in time to descend decreases by close to one order of magnitude. Now, is this the case for just the expected improvement function or how would other objective functions compare for this same test case? In Table 4, each of the different objectives considered (mean, mean minus one standard deviation, mean minus two standard deviations, and expected improvement) all result in a reduction in standard deviation in time to descend to approximately one second.

Table 4: Comparison of Objectives using 10 Samples at 50 Locations when Adding 12 High Fidelity Points

Objective	$\sigma(t_d)$
μ	0.9698
$\mu - \sigma$	1.0686
$\mu - 2\sigma$	0.9272
EI	1.0379

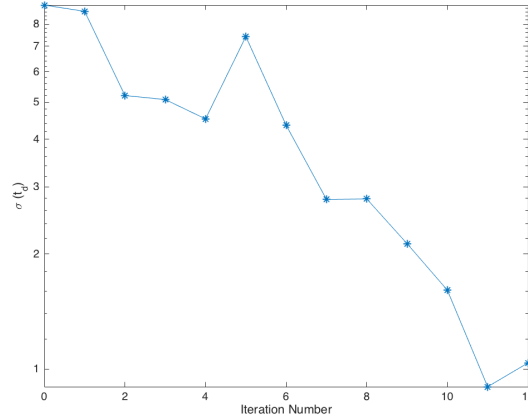


Figure 4: Standard Deviation of Time to Descend using EI objective with 10 MC samples at 50 locations

These results are just for running the algorithm sequentially once. Since we are dealing with a stochastic function, however, we really need to consider how well the algorithm works when run multiple times to test the effectiveness in general. To see the spread for the final time to descend for differing objectives along with different number of locations and Monte Carlo samples at those locations, Table 5 is created by repeating the placement of 5 high fidelity samples 10 times.

Table 5: Comparing Objectives and Number of LHS Locations on QoI

Locations	Samples	μ		$\mu - \sigma$		$\mu - 2\sigma$		EI	
		μ	σ	μ	σ	μ	σ	μ	σ
10	10	3.9463	2.1059	5.7488	2.9285	3.8331	1.3915	7.9923	7.5699
20	20	2.6886	1.4337	6.0775	5.0735	8.1739	10.345	3.7993	2.0152
40	40	2.6559	1.8320	1.7752	0.5261	2.0221	0.9478	2.8685	1.6587

Looking at the results, we see the expected trend where the more samples and location used, the lower the resulting mean and standard deviation uncertainty in time to descend. We do see there are some results where the uncertainty is larger than the mean time to descend. This occurs when the vehicle cannot trim or finds a very slow descent angle. As such, the time to descend on that one case might significantly impact the standard deviation in time to descend. To avoid this problem, we thought to use the 90% confidence interval as our objective instead. In addition, it was thought the confidence interval might converge to its limit using less Monte Carlo samples than the standard deviation in time to descend. Figure 5 shows how the standard deviation changes for an increasing number of MC samples while Figure 6 shows the same plot for the 90% confidence interval.

From these convergence plots, we see that the confidence interval is very close to its limit after approximately 1000 MC samples while the standard deviation needs closer to 10,000 samples. As such, we will use the 90% confidence interval for the rest of our analysis.

Going back to the major decisions mentioned in Section IV, we want to determine how to spread the total number of Monte Carlo samples between additional number of locations and increased number of samples at each location. To conduct this study, we added five high fidelity point sequentially, running the analysis 100 times to generate the statistics. If the confidence interval came back at more than 40 seconds, the result was removed as this was approximately a 10 second increase over the initial starting case and not indicative of the aerodynamic database, but instead of a vehicle that could not be trimmed. This was approximately one or two samples per 100 trials. We first did a study using a total of 1000 MC samples split between locations and samples per location for each of the four different objectives outlined above. The range considered was from 100 samples at each of 10 locations to 10 samples at each of 100 locations. The results are shown in

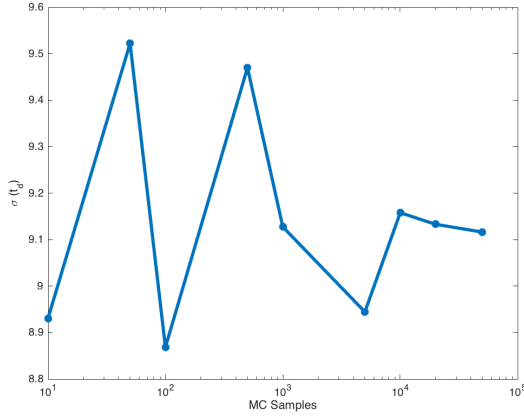


Figure 5: Standard Deviation Convergence with Increasing MC Samples

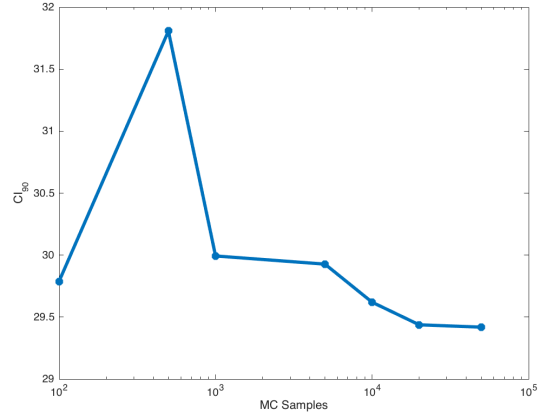


Figure 6: 90% Confidence Interval Convergence with Increasing MC Samples

Table 6.

Table 6: Comparing Objectives, MC samples, and LHS Locations on 90% Confidence Interval

Samples	Locations	μ		$\mu - \sigma$		$\mu - 2\sigma$		EI	
		μ	σ	μ	σ	μ	σ	μ	σ
100	10	13.739	8.2440	14.758	8.9493	15.698	9.0225	13.160	7.4466
50	20	10.930	5.8600	9.8336	5.5472	11.604	7.6092	12.347	7.8607
40	25	10.551	7.8328	11.315	6.9012	11.068	6.9046	10.300	6.1116
25	40	11.588	8.9652	9.3695	5.3484	10.162	6.8444	8.7514	6.0133
20	50	9.1688	6.6414	9.1297	5.8456	9.0596	6.5546	9.2403	6.4712
10	100	10.530	7.9506	10.041	7.1733	10.290	7.1455	11.487	7.6074

When comparing how to split up the total number of MC samples between samples at a location and number of locations, Table 6 shows the best performance, lowest mean and lowest variance, occurs somewhere in the middle between 100 samples - 10 locations and 10 samples - 100 locations. These best results usually occurred when more locations and less samples were used, but at some point, it was better to have more samples than additional locations. To better understand where the optimal breakdown should occur, we conducted a study for two of the objective functions, mean minus two standard deviations and expected improvement, for a larger set of sample-location combinations. We used a number of MC samples between 15 and 35 samples at the number of locations chosen to be as close to 1000 MC samples as possible. The result of this analysis along with the results from Table 6 are plotted in Figure 7 showing the mean 90 % confidence interval and Figure 8 showing the standard deviation of the 90 % confidence interval both after adding 5 high fidelity samples.

Quadratic fits of the points on the log number of locations versus confidence interval are also shown to see how the different objectives affect the optimal number of locations. From these results, we see the best results for our algorithm are obtained in the 40-50 location range when looking at running the algorithm 100 times. To see how these results are impacted by the number of times placing the points, we conducted a study looking at between 10 and 1000 runs to see the impact. Table 7 shows how the number of times running the analysis results in a change in the resulting spread of the mean and standard deviation 90% Confidence Interval using 20 MC samples at each of 50 different locations replacing any results where the confidence interval was larger than 40 seconds.

From this convergence study, most of the results are in the same general range for the mean and standard deviation. As such, using 100 runs is a reasonable number of cases when factoring in the computational cost required to generate a higher number of analysis runs. With the results shown here in the deterministic case,

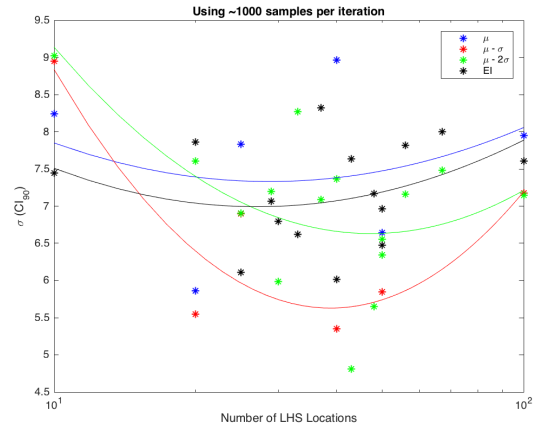
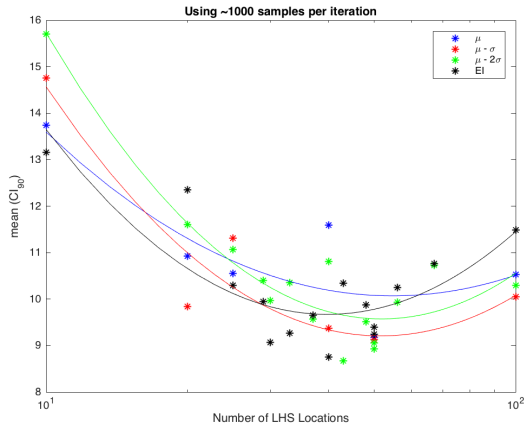


Figure 7: Mean of the 90% Confidence Interval Adding 5 Samples
 Figure 8: Standard Deviation of the 90% Confidence Interval Adding 5 Samples

Table 7: Convergence Study of Number of Times Running Analysis for Different Objectives

Analysis Runs	μ		$\mu - \sigma$		$\mu - 2\sigma$		EI	
	μ	σ	μ	σ	μ	σ	μ	σ
10	9.0211	6.1231	8.4107	5.8580	11.927	5.7570	7.8953	5.3964
20	9.7522	4.4599	7.7018	6.2375	8.4666	4.8602	10.833	8.1086
50	8.6584	5.4772	9.0874	6.8399	9.5035	7.2148	7.8814	4.7497
100	10.124	7.5246	8.9146	5.9018	10.381	7.0120	11.075	7.7780
200	9.6524	6.8042	9.2491	5.7243	10.096	6.8174	9.7641	9.2165
500	10.521	6.9827	10.095	7.0478	9.6158	6.9605	9.8802	6.5512
1000	10.106	7.1387	9.5984	6.5706	9.9082	6.6171	9.9431	6.7090

we think our algorithm shows promise to find a better set of flight conditions to analyze compared to using the total number of high fidelity samples in a predetermined LHS arrangement.

B. Stochastic Vehicle Analysis

For the initial sample updating procedure, we assumed the vehicle had known characteristics and the uncertainty was totally contained in the aerodynamic analysis. During conceptual design, there is uncertainty in the configuration as well as the aerodynamic analysis.

In our first analysis,² we assumed that we knew the idle throttle setting and the maximum torque of each spoiler exactly. Providing information on how these design choices will affect the end probability for meeting certification requirements is something not currently available during conceptual design. Using the stochastic aerodynamic database for the deterministic vehicle analyzed above without adding new high fidelity samples, we ran a set of different cases where we varied the idle throttle setting and maximum torque of the spoiler (τ_{max}). These results are shown in Table 8.

Table 8: Calculating the Mean and Standard Deviation of the Time to Descend for Varying Idle Throttle and Maximum Torque

Idle Throttle	τ_{max}	Mean	Standard Deviation
0.1	3e3	143.6491	12.9669
0.1	5.5e3	124.6757	6.8460
0.1	8e3	125.9083	6.8717
0.15	3e3	167.7098	17.7384
0.15	5.5e3	141.7589	9.1273
0.15	8e3	144.0098	9.2487
0.2	3e3	200.1479	25.2592
0.2	5.5e3	165.5769	12.8692
0.2	8e3	167.9308	12.6840

Looking at these results, we see that the throttle setting has a greater impact on the time to descend than the maximum torque setting. Increasing the maximum torque significantly will not have a dramatic impact as we have specified the maximum throw corresponding to a maximum deflection of 60 degrees for each of the spoilers. The idle throttle setting could potentially either make the CRM be very close to meeting the descent requirement or not depending on what level is deemed appropriate due to other design decisions and engine characteristics.

In addition to varying the throttle and torque setting, the mass of the aircraft and the corresponding moment of inertia (I_{yy}) are not definitively known in conceptual design. It is usually reasonable to estimate the mass of the aircraft is known within approximately 5% during the conceptual design phase. We assume mass is a normal random variable with mean of 545,000 lbs and standard deviation of 13,600 lbs while I_{yy} is normal with mean $2.4e7 \text{ slugs} - ft^2$ and standard deviation of $5e5 \text{ slugs} - ft^2$. Figure 9 shows a histogram of the descent times with varying mass and moment of inertia using 1 control point for both the M_{MO} and V_{MO} segments. It is assumed there is a perfect correlation between the mass and moment of inertia at present. To see how this variance in the weights of the aircraft will affect the end maneuver time, Figure 10 shows how the mass and moment of inertia affect the time to descend.

To help compare Figure 3 and Figure 9, Table 9 is created to show how uncertainty in the mass, torque, and moment of inertia affect the time to descend for a 0.15 throttle setting with V_{MO} and M_{MO} as specified previously.

Looking at the results in Figure 10 along with Table 9 we see that there does not seem to be a significant increase in time to descend due to the moment of inertia, mass or spoiler torque. This does not mean that these parameters, if assumed constant, will not affect the results of our optimization.

C. Stochastic Vehicle Optimization

After we have looked to see how the vehicle uncertainty impacts the descent time of the initial vehicle, the impact of the vehicle uncertainty on the placement of points should be completed. To do this, Table 10

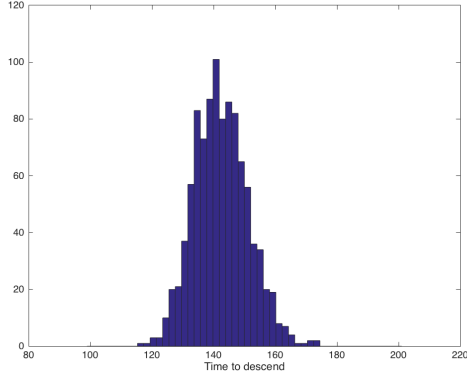


Figure 9: Histogram of Descent Times

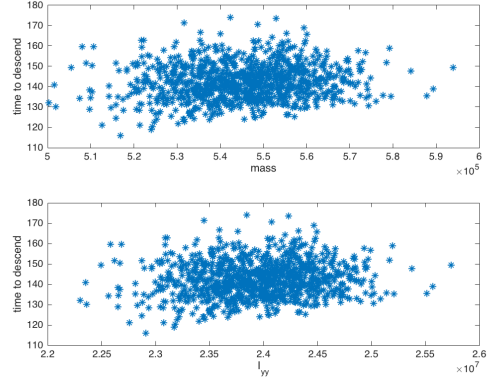


Figure 10: Effect of Mass (top) and Moment of Inertia (bottom) on Descent Time

Table 9: Effect of Uncertain Characteristics on Descent Time

Mass	I_{yy}	τ_{max}	Mean	Standard Deviation	$CI_{90\%}$
[lbs]	[slugs - ft ²]	[ft-lbs]	[sec]	[sec]	[sec]
545e3	2.4e7	5.5e3	141.7589	9.1273	29.9647
$N(545e3, 136e2)$	$N(2.4e7, 5e5)$	5.5e3	142.4485	8.7685	28.8191
545e3	2.4e7	$N(5.5e3, 5.5e2)$	142.0462	8.9858	29.4634
$N(545e3, 136e2)$	$N(2.4e7, 5e5)$	$N(5.5e3, 5.5e2)$	142.0314	8.8503	29.4894

is created to show how the resulting 90% confidence interval changes for uncertainty in different vehicle components for 20 analysis runs using 20 samples at 50 locations for the mean and EI objectives.

Table 10: Effect of Vehicle Uncertainty on Algorithm Performance

Uncertainty	μ		EI	
	μ	σ	μ	σ
Aero-Only	9.5722	4.4599	10.833	8.1086
Mass- I_{yy}	11.614	7.1074	12.016	7.7579
Spoiler	7.3501	3.9943	8.6229	4.1839
Mass- I_{yy} -Spoiler	10.020	4.6084	13.696	8.4102

This table shows the uncertainty in the vehicle does not have a drastic effect on the performance of our methodology for the mean or EI objectives. It seems the mass- I_{yy} uncertainty potentially has a greater impact on the algorithm than the spoiler uncertainty. Comparing the results of Table 10 with the spread of points in Table 7, the uncertainty we added to the vehicle does not seem to have a dramatic impact. As such, our methodology is extendable to dealing with stochastic vehicles, but further testing is necessary to understand what additional limitations might need to be put in place.

VI. Summary & Conclusions

Throughout this paper, we first recapped a methodology to use in conceptual design to analyze certification maneuvers and then presented a new algorithm that identifies the flight conditions that should be evaluated using additional samples of the high fidelity information source. This methodology to determine the best location to sample incorporates one set of Gaussian Processes to build the stochastic database and a second to connect flight conditions to the quantity of interest. In order to use this methodology, we had to

make a decision on what objective function of the QoI, such as the mean or expected improvement, to optimize over. Determining the number of MC samples to run using the aerodatabase updated with the mean of the Gaussian Process at a chosen number of LHS locations in the domain was also necessary. We found that it is best to use a larger number of locations and less samples per locations to improve performance, but as the number of MC samples reduces, the uncertainty increases and the performance degrades. The objectives analyzed did not have a significant impact on the performance of the updating procedure.

While uncertainty in the vehicle did not have a dramatic impact on the performance of our algorithm, in future, it would be interesting to see how uncertainty in the aerodynamic database at the high fidelity sampling locations would impact the results. In addition, we use the mean to represent the aerodynamic characteristics at the LHS locations, but the mean is only the best estimate, not the actual result. As such, the Gaussian Processes connecting the sampling locations to the QoI should have some uncertainty at the locations specified. When considering uncertainty in the vehicle, we saw that the idle throttle setting had the largest impact on the time to descend. With these results, the engineers have a quantifiable estimate of the impact on maneuvers of interest compared to design decisions and can make corresponds trades to improve the configuration or mitigate risk in aircraft conceptual design.

Acknowledgments

The authors would like to thank The Boeing Company for funding this research under grant number 115393 [IC2014-0547]. Also, Brian Whitehead for his insight.

References

- ¹Norris, G., “787-9 Test Lessons to Aid 787-10 and 777X,” aviationweek.com/commercial-aviation/787-9-test-lessons-aid-787-10-and-777x, October 2014.
- ²Wendorff, A. D., Alonso, J. J., and Bieniawski, S. R., “A Multi-Fidelity Approach to Quantification of Uncertainty in Stability and Control Databases for use in Stochastic Aircraft Simulations,” *16th AIAA/ISSMO Multidisciplinary Analysis and Optimization Conference*, AIAA 2015-3439, June 2015.
- ³Lophaven, S., Nielsen, H., and Søndergaard, J., “Aspects of the Matlab Toolbox DACE,” Tech. Rep. 2002-13, Informatics and Mathematical Modelling.
- ⁴Huang, D., Allen, T. T., Notz, W. I., and Miller, R. A., “Sequential Kriging Optimization Using Multiple Fidelity Evaluations,” *Structural and Multidisciplinary Optimization*, Vol. 32, No. 5, November 2006, pp. 369–382.
- ⁵Federal Aviation Administration, *Section 25.841 - Pressurized Cabin*, January 1999.
- ⁶Stevens, B. L. and Lewis, F. L., *Aircraft Control and Simulation*, John Wiley & Sons, Inc., 2nd ed., 2003.
- ⁷Stoecklin, R. L., “Development, Manufacturing, and Test of Graphite-Epoxy Composite Spoilers for Flight Service on 737 Transport Aircraft,” Tech. Rep. 132682, NASA, 1976.
- ⁸Vassberg, J. C., DeHaan, M. A., Rivers, S. M., and Wahls, R. A., “Development of a Common Research Model for Applied CFD Validation Studies,” *AIAA*, AIAA 2008-6919, 2008.
- ⁹“777-200/300 Characteristics for Airport Planning,” Tech. Rep. D6-58329, Boeing Commercial Airplanes, July 1998.
- ¹⁰Bunge, R. A. and Kroo, I. M., “Compact Formulation of Nonlinear Inviscid Aerodynamics for Fixed-Wing Aircraft,” *AIAA Applied Aerodynamics Conference*, AIAA 2012-2771, June 2012.
- ¹¹Tang, C. Y., Gee, K., and Lawrence, S. L., “Generation of Aerodynamic Data using a Design of Experiment and Data Fusion Approach,” *AIAA Aerospace Sciences Meeting*, AIAA 2005-1137, January 2005.
- ¹²Jones, D. R., Schonlau, M., and Welch, W. J., “Efficient Global Optimization of Expensive Black-Box Functions,” *Journal of Global Optimization*, Vol. 13, June 1998, pp. 455–492.